Mechanics and Mechanical Engineering
Vol. 22, No. 2 (2018) 509–519

https://doi.org/10.2478/mme-2018-0041

Influence of the Diffuser on the Drag Coefficient of a Solar Car

Paula Mierzejewska
Artur Cieśliński
Daniel Jodko
Institute of Turbomachinery
Lodz University of Technology
Lodz, Poland
221885@edu.p.lodz.pl
artur.cieslinski0@gmail.com
daniel.jodko@p.lodz.pl

Received (23 June 2018)
Revised (19 August 2018)
Accepted (13 September 2018)

The purpose of the research was to design a solar vehicle for Bridgestone World Solar Challenge competition which takes place biannually in Australia. The article, however, presents the aerodynamic research on the car body, especially on the exit diffuser. Numerous CFD simulations of different diffuser shapes were performed in ANSYS CFX software. The paper presents the results of pressure distribution on the body and velocity contours. The drag force acting on the car body is dependent on the pressure distribution. The article includes comparison of corresponding drag coefficient values for different cases. Furthermore, the variation of the lift force depending on the shape of the bodywork was also taken into consideration. The research shows that slight differences in the construction of the exit diffuser correspond to noticeable changes in the drag coefficient values (0.138 minimum, 0.168 maximum) and significant changes in the lift force (minimum 71 N, maximum 160 N).

Keywords: drag coefficient, numerical simulation, solar car, aerodynamics, drag force.

1. Introduction

Lodz Solar Team, a student scientific association of Lodz University of Technology, established a scientific-research project whose aim was to design and build a solar urban vehicle for the sake of Bridgestone World Solar Challenge competition, taking place biannually in Australia. Lodz Solar Team constructed the first Polish solar vehicle called Eagle One, which participated in the competition in 2015. Change of the regulations for the 2017 edition required a construction of a new model, Eagle Two. Due to the fact that the main goal was to minimize energy consumption, it

was of particular significance to design a car body of minimum possible drag force as well as meeting the regulations requirements.
In case of a viscous flow past a body (or a body moving in a viscous fluid) an aerodynamic force acting on a body has to be considered. Depending on the object shape, force acting on the object due to flow may act in different directions. It consists not only of drag force – but it is resolved into two components – horizontal (drag force) and vertical (lift force) (Figure 4). Hence, the formula for total aerodynamic force acting on a body moving in a fluid is equal [1,2]:

$$\overrightarrow{F_a} = \overrightarrow{F_{a_{drag}}} + \overrightarrow{F_{a_{lift}}}$$

where: $F_{a_{drag}}$ – aerodynamic drag, $F_{a_{lift}}$ – aerodynamic lift.
As far as drag forces acting on a vehicle in the direction of motion are concerned, two components have to be considered – rolling friction and aerodynamic drag [3]:

$$F_{drag} = F_{friction} + F_{a_{drag}}$$

where: $F_{friction}$ – rolling friction force, F_{adrag} – aerodynamic drag.
Both of these components are dependent on the forces acting on a car body due to relative motion with fluid. The friction force is dependent on the generated lift force. The formula for the friction force is equal [3]:

$$F_{friction} = f\,N = f\,(F_g - F_{a_{lift}})$$

where: f – rolling friction coefficient, N – normal force (dependent on gravity and lift force).
Aerodynamic drag force is acting reversely to the object movement direction. A normal force proportional to the static pressure and tangential force proportional to tangential stress acts on each element of that object [5]. After calculation of resultant forces on the whole body surface and their projection on velocity vector direction there is obtained aerodynamic drag $F_{a_{drag}}$ (due to friction (viscosity) and surface pressure distribution), which is dependent on the shape and roughness of the body and the Reynolds number [1, 4]:

$$F_{a_{drag}} = F_{a_{drag1}} + F_{a_{drag2}}$$

where: $F_{a_{drag1}}$ – aerodynamic drag due to friction (viscosity), $F_{a_{drag2}}$ – aerodynamic drag due to surface pressure distribution.
The action of friction and pressure drag on an object is presented in the Figure 1.
Aerodynamic drag due to friction is caused by the fact that the body moving in a fluid propels adjacent fluid layers. The layers directly adhering to the body move with velocity of that body, whereas further layers are also propelled but they are moving with slower velocities which causes friction. Such drag is dominant for low Re cases, in particular for flows characterised by $Re < 1$. The formula for friction drag is as follows [1]:

$$\overrightarrow{F}_{a_{drag1}} = \int_A \tau\,\overrightarrow{t}\,dA$$

where: τ – tangential stress, $\overrightarrow{t}$ – unit tangential vector, A – area.

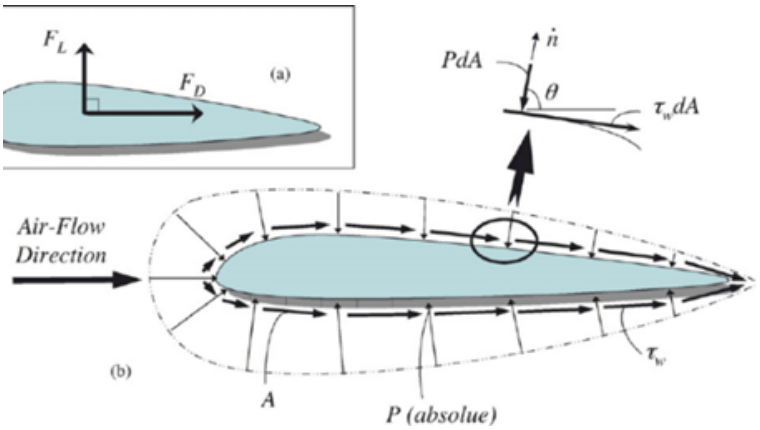

Figure 1 Drag force acting on a body [1]

On the other hand, the pressure drag F_2 is a result of pressure difference between the front and the rear of the body, which is due to the changing flow velocity around the body – when flow is decelerating the static pressure increases and when the flow is accelerating the static pressure decreases. The drag due to pressure distribution is overbearing at higher Reynolds numbers ($Re > 1$). The formula for pressure drag is as follows [1]:

$$\overrightarrow{F}_{a_{drag2}} = -\int_A P\overrightarrow{n}\,dA$$

where: P – pressure, $\overrightarrow{n}$ – unit normal vector, A – area.
The formula for the total drag is, hence, as follows:

$$\overrightarrow{F}_{a_{drag}} = \int_A \left(\tau\overrightarrow{t} - P\overrightarrow{n}\right) dA$$

The value of aerodynamic drag force can also be calculated according to the following equation [5]:

$$F_{a_{drag}} = \frac{1}{2}\rho S c_x v^2$$

where: ρ – fluid density, S – frontal area, c_x – drag coefficient, v – velocity.
The transformation of the above equation allows easy determination of the drag coefficient value knowing the rest of the variables.

2. Researched models

The research includes comparison of four Eagle Two vehicle concepts. The dimensions of the models are 4.95 m × 1.60 m × 1.30 m (length × width × height). The area of the roof is restricted by the competition regulations and is corresponding to 5 m^2 of photovoltaic cells. The shape of the rear and the diffusor is different for particular models.

The view of the model ASP11 is presented in the Figure 2. The frontal area of all four models is equal to 1.61 m^2. The models prepared for the simulations were simplified versions of the vehicle construction. The geometry included car body and wheels, however, more complex elements of the construction such as suspension, gaps between bodywork elements and other body irregularities were neglected due to limitations of the software ANSYS CFX.

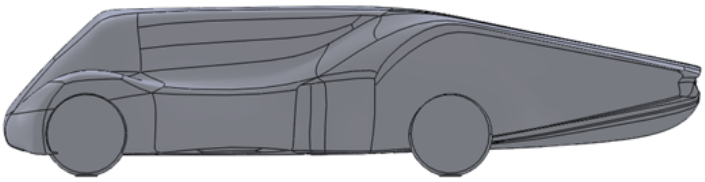

Figure 2 The shape of vehicle model ASP11

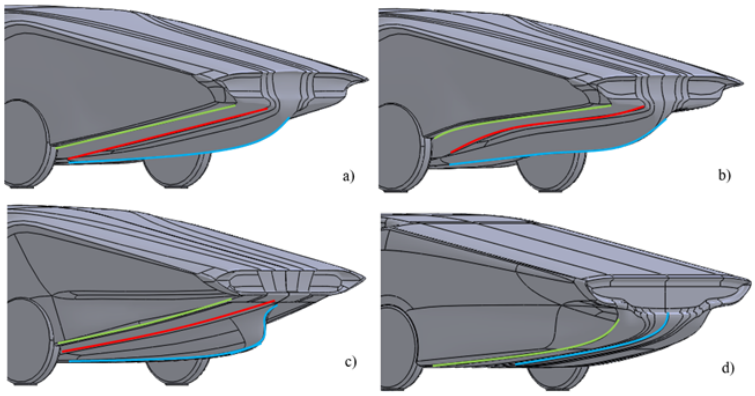

Figure 3 Diffusor shapes (a – model ASP11, b – model ASP12, c – model ASP13, d – model ASP18)

Investigated solar vehicle models are designed with different shapes of diffusor. The diffuser variation was performed in order to optimize aerodynamic drag of the vehicle and its energy consumption. The shapes of four of the investigated diffusors are presented in the Figure 3.

As it is visible in the Figure 3a,b the models ASP11 and ASP12 have very similar construction of the rear (Figure 3a, b). The dimensions of the fin are the same, however, the shape of the diffusor is different. In case of ASP 11 the generatrix of the diffuser is straight, whereas in case of ASP 12 it is rapidly diverging in the first stage and slowly diverging in the second stage.

Similarly to previous cases the model ASP 13 (Figure 3c) consists a fin, however of significantly different shape. The last model, ASP 18 (Figure 3d), is a simple diffuser, but converging in horizontal cross-section of a car as well.
The idea of each design was to distribute flow evenly on the rear part of the car, so that the pressure could be recovered and drag was lowered.

3. Assumptions and setup

The simulations were performed in the ANSYS CFX. The geometry includes aerodynamic tunnel in which a vehicle model is placed. The dimensions of the tunnel are 40 × 10 × 12 m (length × width × height) (Figure 4).

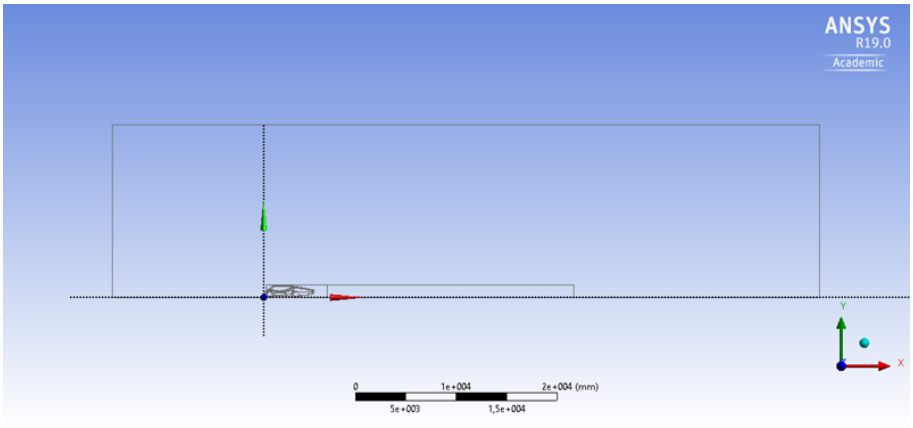

Figure 4 Geometry of the tunnel

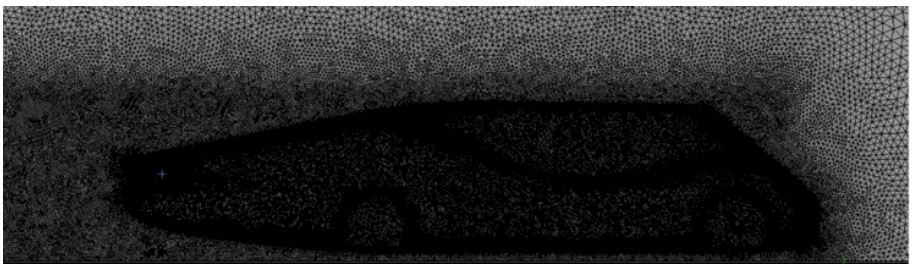

Figure 5 Mesh around the vehicle

For the purpose of mesh concentrating there were also created volumes containing the car model and directly behind it. The tunnel was meshed using patch conforming method with tetrahedrons (Figure 5). There was applied body sizing on crucial volumes and surface sizing and inflation layers on the car model surfaces.

As far as setup is concerned, the following conditions were applied:

- Domain: Air Ideal Gas (Continuous Fluid),
- Heat transfer option: Isothermal,
- Fluid temperature: 25^{o}C,
- Flow model: Stationary
- Turbulence model: Shear Stress Transport.

The concept of the research is based on the simulation of the stationary vehicle in a tunnel with flowing fluid, hence the following conditions were applied in order to simulate real-life conditions:

- Inlet normal speed: 70 km/h (considered vehicle speedy),
- Outlet relative pressure: 0 Pa (reference pressure: 1 atm),
- Wheels: No slip wall, Rotating Wall (corresponding to the velocity of vehicle),
- Road: No slip wall, wall velocity (considered vehicle speed),
- Car body: Smooth Wall, No Slip Wall,
- Symmetry condition (half of the geometry was simulated due to the hardware limitations).

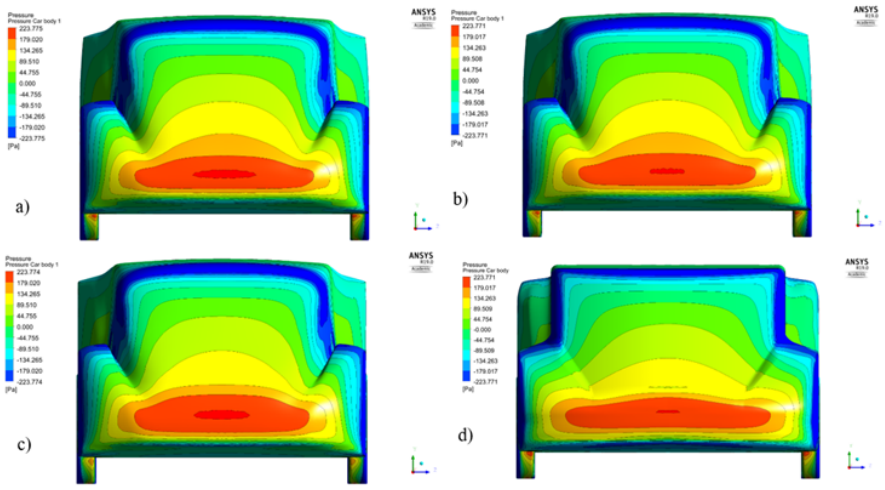

Figure 6 Static pressure distribution at the front of vehicles (a – model ASP11, b – model ASP12, c – model ASP13, d – model ASP18)

4. Results

The value of the drag force and drag coefficient for Re > 1 is dependent mainly on the recovery of the static pressure. It is of particular significance that the maximum of the static pressure at the front of the vehicle is regained at the diffusor and the rear. The static pressure distribution at the front of each model is presented in the Figure 6. It is clearly visible that the distribution is similar for all four models.
The static pressure distribution on the rear and bottom of each car model is presented in the Figure 7 and Figure 8. It is clearly visible that the distribution is significantly different in all four cases. The flow structure changes under the body and the recovery of static pressure occurs in different manner. It is noticeable that even a small change in the shape of the diffusor (model ASP11 and ASP12, Figure 7 a, b) causes major changes in the behaviour of the fluid flow past the vehicle and, hence the static pressure distribution differs considerably.

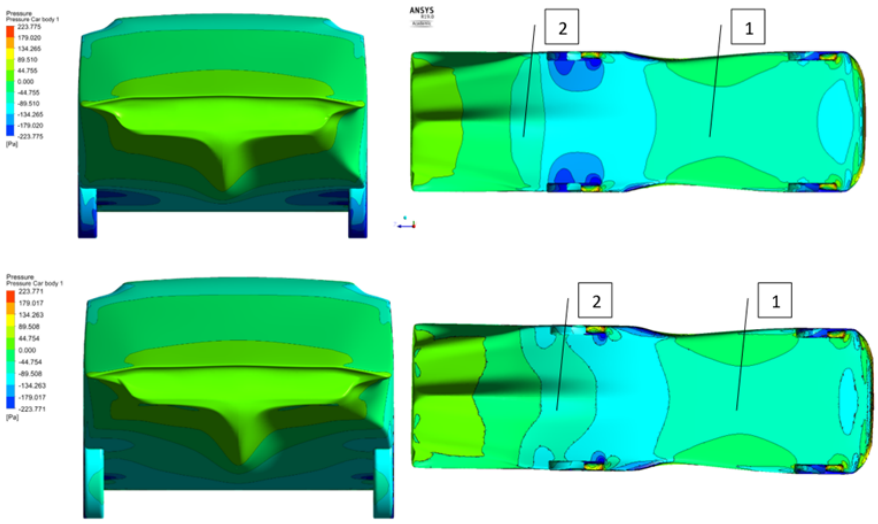

Figure 7 Static pressure distribution at the rear and bottom (a – model ASP11, b – model ASP12)

The region 1 of models ASP 11 and ASP 12 show areas with decreased pressure, so the flow there is accelerated. Conclusion can be drawn that the flow in this diffuser part is more unstructured what influences pressure recovery. Whereas, in case of models ASP 13 and ASP 18 show the pressure in the region 1 is higher, hence the flow does not accelerate so much.
The region 2 in the diffuser part shows different phenomenon. In ASP 11 and ASP 12, transitions between pressure contours are curvy (it means there are no straight lines perpendicular to the symmetry axis of the car/free-stream direction of the flow), so the conclusion can be drawn that the velocity changes randomly there. In result, there are transverse velocity gradients, and the flow is mixing in this region, so the turbulences are created, and less pressure is recovered. In contrast,

ASP 13 and ASP 18 displays striped pressure zones. They are perpendicular to the symmetry axis, so the velocities of the particles are similar, and there is no mixing due to the transverse velocity gradients. It suggests higher recovery of the static pressure in case of these models.

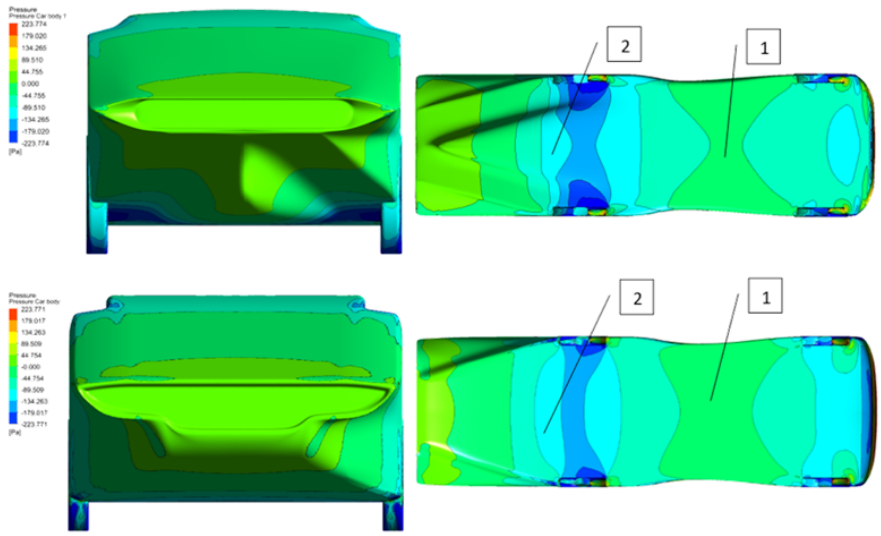

Figure 8 Static pressure distribution at the rear and bottom (a – model ASP13, b – model ASP18)

Figures 9 and 10 present velocity contour for four researched models. In every case there is no visible flow separation in both upper and lower part of the rear, what results in rather low drag coefficient comparing to casual cars. Also, in every concept flow structure is very similar – low velocity point in the very front, high-velocity point at the top of the front window, and flow attached to the rear part

The flow structures differ mainly in the rear and behind the car. In region 3 flow is accelerated for ASP 11 and ASP 12 (Figure 9a, b), which influence the structure of turbulences in the diffuser. The centre of generated eddy (region 4) is moved to the upper part of the car, so the flow underneath and above the rear are not symmetrical. This means that significant amount of the flow energy is dissipated in the eddy.

On the other hand, models ASP 13 and ASP 18 (Figure 10a, b) display slightly lower velocity under the car (region 3), which results in more efficient flow distribution in the diffuser. Due to the fact that the centre of the eddy generated in region 4 is moved into half of the height of the rear vertical wall (the separation region), the eddies are more symmetrical, so less energy is dissipated, and lower drag is generated.

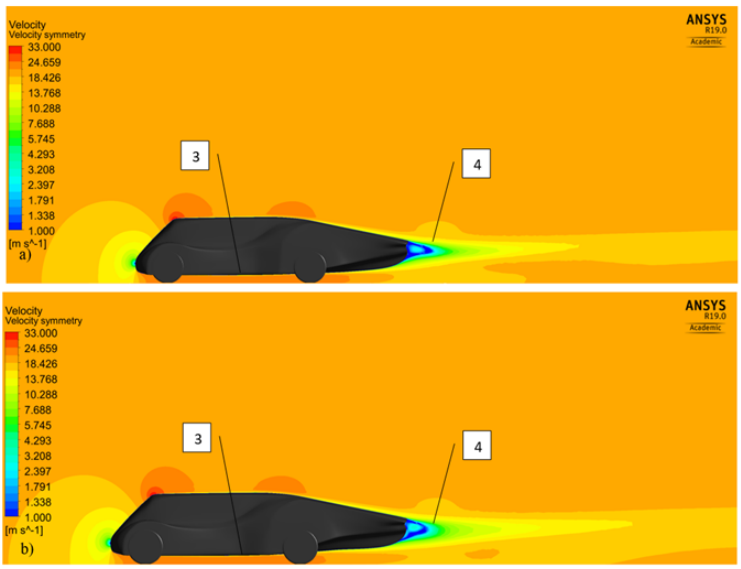

Figure 9 Velocity contour (a – model ASP11, b – model ASP12)

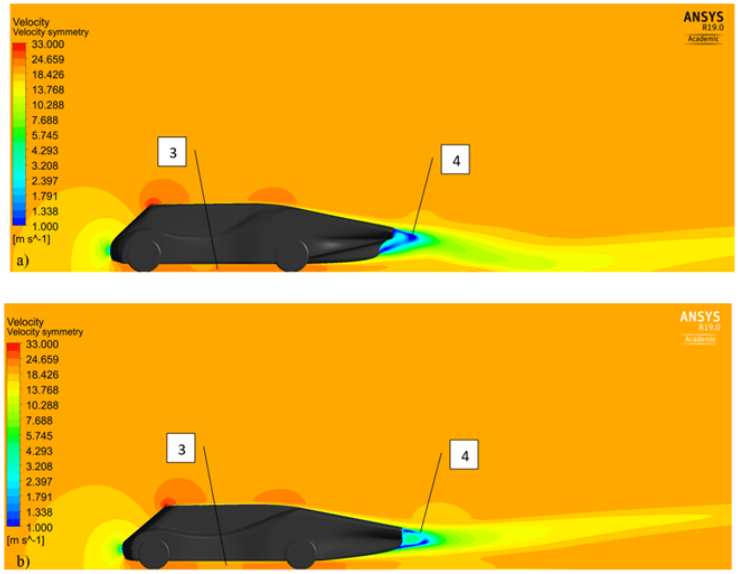

Figure 10 Velocity contour (a – model ASP13, b – model ASP18)

Table 1 presents gathered results for the researched models. All four vehicle models were tested for the velocity equal to the 19.44 m/s (70 km/h). As far as lift force is concerned, in all cases it is negative, which means there occurs a downforce. The smallest value of downforce is equal 71 N and is observed for model ASP 12 (on the other hand, very similar model ASP 11 provides the highest value of the down force amongst all cases, equal to 160N).

Table 1 Results from Ansys Workbench

Model	ASP 11	ASP 12	ASP 13	ASP 18
Velocity [km/h]	70	70	70	70
Frontal Area [m^2]	1.61	1.61	1.61	1.61
Aerodynamic Lift Force [N]	-159.9	-71.0	-123.8	-130.2
Aerodynamic Drag Force [N]	56.0	60.7	55.2	50.0

Taking into consideration drag force, it is noticed that the smallest value is equal 50 N and is obtained for ASP 18 model. The highest drag force value corresponds to ASP12 model and is equal 60.7 N. The corresponding drag coefficient values are presented in the Table 2.

Table 2 Drag coefficient

Model	ASP 11	ASP 12	ASP 13	ASP 18
Drag Coefficient [-]	0.156	0.168	0.144	0.138

Since the mass of the vehicle was predicted to be approximately 350 kg and the tyres friction coefficient was claimed by the manufacturer to be $f = (0.0013 \div 0.0040)$ the maximum value of rolling friction drag (for ASP 11) is equal 14,64 N (the majority of which corresponds to the mass of the vehicle). Hence, the value of the lift force does not have such high impact on the energy consumption as the aerodynamic drag force. Therefore, it was sought for further drag coefficient minimization.

5. Conclusions

In conclusions, the article presents part of the research concerning solar vehicle aerodynamics. There were presented four designed models with different shapes of diffusors – three with tail fin (two of them very similar) and one without trail fin. The purpose was to design a body that would result in even flow distribution on the rear part, better pressure recovery, and thus, lowered drag.
As it was presented in the Table 2, the drag coefficient values obtained for researched models are similar and significantly lower than in case of most urban vehicles.
As it was visible in the Figures 6-10, the behaviour of the flow changes in all four cases. It was noticed, that very small changes in the geometry of the diffuser (the generatrix) in case of models ASP 11 and ASP 12 led to significant changes in the results. The value of the lift force dropped from its maximum (for ASP 11) to its minimum (ASP 12), whereas the drag coefficient increased noticeably.

According to the results, the performed changes (rear part of the tail fin) when designing ASP 13 model allowed decreasing the drag coefficient value by 7.7% (0.144). However, the value of obtained drag did not satisfy the designers, hence the next step was to simulate the model without the tail fin, however, with diffuser shape resembling the fin from ASP 11 model (model ASP 18). According to the calculation the model is characterised by the lowest drag coefficient equal to 0.138. The research in total included simulation of over 60 models and the results obtained for model ASP 18 were the most satisfying. Hence, it was the shape of model ASP 18 that was applied during building of Eagle Two vehicle.

References

[1] **White, F. M.**: Fluid mechanics, , *5th. Boston: McGraw-Hill Book Company, Boston*, **2003**.

[2] **Jeżowiecka-Kabsch, K., Szewczyk, H.**: Mechanika płynów, *Oficyna Wydawnicza Politechniki Wrocławskiej, Wroclaw*, **2001**.

[3] **Anderson, R.**: Online estimation of rolling resistance and air drag for heavy duty vehicles, *KTH Industrial Engineering and Management, Stockholm*, **2012**.

[4] **Kosma, Z.**: Podstawy mechaniki płynów, *Politechnika Radomska, Radom*, **2005**.

[5] **Vennard, J. K.**: Elementary fluid mechanics, *Read Books, Ltd, New Yok*, **2013**.